

Exact radiation trapping force calculation based on vectorial diffraction theory

Djenan Ganic, Xiaosong Gan, and Min Gu

Centre for Micro-Photonics, School of Biophysical Sciences and Electrical Engineering
Swinburne University of Technology, P.O. Box 218, Hawthorn 3122, Australia
mgu@swin.edu.au

Abstract: There has been an interest to understand the trapping performance produced by a laser beam with a complex wavefront structure because the current methods for calculating trapping force ignore the effect of diffraction by a vectorial electromagnetic wave. In this letter, we present a method for determining radiation trapping force on a micro-particle, based on the vectorial diffraction theory and the Maxwell stress tensor approach. This exact method enables one to deal with not only complex apodization, phase, and polarization structures of trapping laser beams but also the effect of spherical aberration present in the trapping system.

© 2004 Optical Society of America

OCIS codes: (260.1960) Diffraction theory; (110.0180) Microscopy; (140.7010) Trapping

References and links

1. A. Ashkin, J. M. Dziedzic, and T. Yamane, "Optical trapping and manipulation of single cells using infrared laser beams," *Nature* **330**, 769-771 (1987).
2. A. Ashkin, K. Schütze, J. M. Dziedzic, U. Euteneuer, and M. Schliwa, "Force generation of organelle transport measured in vivo by an infrared laser trap," *Nature* **348**, 346-348 (1990).
3. S. Chu, "Laser manipulation of atoms and particles," *Science* **253**, 861-866 (1991).
4. D. Ganic, X. Gan, and M. Gu, "Generation of doughnut laser beams by use of a liquid-crystal cell with a conversion efficiency near 100%," *Opt. Lett.* **27**, 1351-1353 (2002).
5. V. R. Daria, P. J. Rodrigo, and J. Glückstad, "Dynamic array of dark optical traps," *Appl. Phys. Lett.* **84**, 323-325 (2004).
6. W. M. Lee and X. C. Yuan, "Observation of three-dimensional optical stacking of microparticles using a single Laguerre-Gaussian beam," *Appl. Phys. Lett.* **83**, 5124-5126 (2003).
7. M. P. MacDonald, L. Paterson, K. Volke-Sepulveda, J. Arlt, W. Sibbett, and K. Dholakia, "Creation and manipulation of three-dimensional optically trapped structures," *Science* **296**, 1101-1103 (2002).
8. D. Ganic, X. Gan, and M. Gu, "Focusing of doughnut laser beams by a high numerical-aperture objective in free space," *Opt. Express* **11**, 2747-2752 (2003).
9. V. Garcés-Chávez, D. McGloin, H. Melville, W. Sibbett, and K. Dholakia, "Simultaneous micromanipulation in multiple planes using a self-reconstructing light beam," *Nature* **419**, 145 (2002).
10. A. Ashkin, "Forces of a single-beam gradient laser trap on a dielectric sphere in the ray optics regime," *Biophys. J.* **61**, 569-582 (1992).
11. J. P. Barton, D. R. Alexander, and S. A. Schaub, "Theoretical determination of net radiation force and torque for a spherical particle illuminated by a focused laser beam," *J. Appl. Phys.* **66**, 4594-4602 (1989).
12. A. Rohrbach and E. H. K. Stelzer, "Optical trapping of dielectric particles in arbitrary fields," *J. Opt. Soc. Am. A* **18**, 839-853 (2001).
13. A. Rohrbach and E. H. K. Stelzer, "Trapping forces, force constants, and potential depths for dielectric spheres in the presence of spherical aberrations," *Appl. Opt.* **41**, 2494-2507 (2002).
14. J. A. Lock, "Calculation of the radiation trapping force for laser tweezers by use of generalized Lorenz-Mie theory. I. Localized model description of an on-axis tightly focused laser beam with spherical aberration," *Appl. Opt.* **43**, 2532-2544 (2004).
15. J. A. Lock, "Calculation of the radiation trapping force for laser tweezers by use of generalized Lorenz-Mie theory. II. On-axis trapping force," *Appl. Opt.* **43**, 2545-2554 (2004).
16. P. Török, P. Varga, Z. Laczik, and G. R. Booker, "Electromagnetic diffraction of light focused through a planar interface between materials of mismatched refractive indices: an integral representation," *J. Opt. Soc. Am. A* **12**, 325-332 (1995).
17. M. Gu, *Advanced optical imaging theory* (Springer, Heidelberg 2000).
18. W. H. Wright, G. J. Sonek, and M. W. Berns, "Radiation trapping forces on microspheres with optical tweezers," *Appl. Phys. Lett.* **63**, 715-717 (1993).

1. Introduction

Optical trapping of micro-particles by a single laser beam focused by a high numerical aperture (NA) microscope objective has become a useful and important tool for manipulation of small objects in many disciplines including physics, chemistry and biological studies [1]. The accurate knowledge of trapping forces is of crucial importance in these applications, for example, in understanding the dynamic performance of microtubule-based organelle motors [2] or the elastic properties of DNA molecules [3]. Recently, spatial phase modulators [4,5], and computer-generated holograms [6] are widely used for generating complex laser beams, such as Laguerre-Gaussian beams, for novel laser trapping experiments [5-7]. Focusing of such beams with a high NA objective required for efficient trapping leads to a complicated amplitude, phase and polarization distributions of an electromagnetic (EM) field in the focal region [8]. Interaction of such a field with a micro-particle results in the controllable laser trapping technique [7,9].

Currently, there are in principle two methods for calculating trapping forces exerted on a spherical micro-particle, each of which has certain limitations and is not adequate to deal with the focal distribution complexity. The first method is based on the ray optics (RO) theory [10]. In this method, the wave nature of a trapping beam cannot be dealt with at all. Therefore, the magnitude of trapping force is independent of particle size and it is valid for large particles (larger than 10λ). The second method is based on the interaction of the fifth-order corrected Gaussian beam with a micro-particle and the Maxwell stress tensor approach [11]. This method indicates that the magnitude of trapping force is particle-size dependent and it is applicable for small particles ($\sim\lambda$ order). However, a fifth-order Gaussian beam ignores the effect of diffraction by a high NA objective and thus does not correctly represent the EM phase and polarization distributions near the focus of a high NA objective (Figs. 1(b) and 1(c)). In addition, neither of the two methods enables us to model the effect of spherical aberration (SA) usually presents during laser trapping experiments due to the refractive index mismatch between the immersion oil (or the coverslip) and aqueous solution in which particles are situated.

Recently, Rohrbach *et al.* [12,13] have developed a method for calculation of trapping forces of an EM wave on an arbitrary-shaped dielectric particle, based on the extension of Rayleigh-Debye theory to include second-order scattering, which considers a stronger interaction between the incident field and the particle. However, this method is limited to the case when the maximum phase shift $k_0(n_s - n_m)2r$ produced by the particle of radius r , is smaller than $\pi/3$. This is valid, for example, for a polystyrene particle in water illuminated by highly focused laser ($\lambda_0 = 1.064 \mu\text{m}$) of radius $r = 370 \text{ nm}$ or less, but for larger particles it would be inaccurate. Generalized Lorenz-Mie theory is another approach that can be used to determine the trapping force in the presence of the spherical aberration, but to date it has only been used to determine the on-axis trapping force [14,15].

In this paper we adopt the vectorial diffraction [16,17] approach to represent the highly focused beam and its interaction with a micro-particle, while the Maxwell stress tensor method is used to calculate the radiation trapping forces on a micro-particle. Such an approach enables one to consider the vectorial properties of the EM field distribution in the focal region of a high NA microscope objective. Effects such as the complex phase modulation, the refractive index mismatch, i.e., SA, the polarization dependence, and the objective apodization can be considered using our model without the loss of generality.

2. Model

A schematic diagram of our model that includes the SA effect is shown in Fig 1(a), where the geometrical focus position defines the origin of our coordinate system, while the position of the particle is defined as the position of its center with respect to the origin. Such situation usually occurs when a dry or an oil immersion objective is used to trap particles suspended in water.

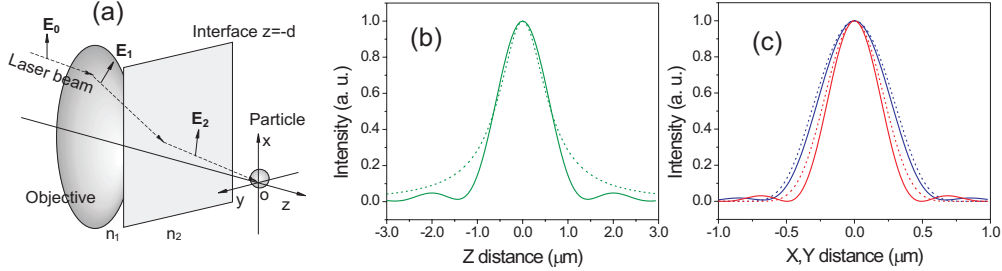


Fig. 1. (a) Schematic of our model. Intensity distribution in (b) axial and (c) transversal directions (blue-X axis, red-Y axis) for the fifth-order Gaussian approximation (dashed line) and the vectorial diffraction theory (solid line).

Using the vectorial Debye theory and considering a linearly polarized monochromatic plane wave focused into two media separated by a planar interface, one can express the electric and magnetic field distributions in the focal region of a high NA objective, if the polarization direction is along the x direction, as [16]

$$\mathbf{E}_2(\mathbf{r}_p, -d) = -\frac{ik_1}{2\pi} \iint_{\Omega_1} \mathbf{c}(\phi_1, \phi_2, \theta) \exp\{ik_0[r_p \kappa + \Psi(\phi_1, \phi_2, -d)]\} \sin \phi_1 d\phi_1 d\theta \quad (1)$$

$$\mathbf{H}_2(\mathbf{r}_p, -d) = -\frac{ik_1}{2\pi} \iint_{\Omega_1} \mathbf{d}(\phi_1, \phi_2, \theta) \exp\{ik_0[r_p \kappa + \Psi(\phi_1, \phi_2, -d)]\} \sin \phi_1 d\phi_1 d\theta. \quad (2)$$

Equations (1) and (2) are given in spherical polar coordinates where indices 1 and 2 refers to the first medium (refractive index n_1) and the second medium (refractive index n_2), respectively. ϕ_1 is the angle of incidence on the planar interface, while ϕ_2 is the angle of refraction. \mathbf{r}_p is the position vector while k_0 and k_1 are wave vectors in vacuum, and the first medium, respectively. The focus depth is denoted by d , while functions $\mathbf{c}(\phi_1, \phi_2, \theta)$, $\mathbf{d}(\phi_1, \phi_2, \theta)$, and κ are defined in Ref. [16]. Function $\Psi(\phi_1, \phi_2, -d)$ is so called the SA aberration function caused by the refractive index mismatching [16], where d represents the focal depth in the second medium. Any other polarization state can be resolved into two orthogonal states each of which satisfies Eqs. (1) and (2).

If we consider a homogeneous microsphere situated in the second medium n_2 illuminated by a monochromatic EM field described by Eqs. (1) and (2), the net radiation force on the microsphere according to the steady-state Maxwell stress tensor analysis is given by [11]

$$\langle \mathbf{F} \rangle = \frac{1}{4\pi} \iint_0^{2\pi} \int_0^\pi \left(\left(\epsilon_2 E_r \mathbf{E} + H_r \mathbf{H} - \frac{1}{2} (\epsilon_2 E^2 + H^2) \hat{\mathbf{r}} \right) \right) r^2 \sin \phi d\phi d\theta, \quad (3)$$

where r, ϕ and θ are spherical polar coordinates, E_r and H_r are the radial parts of the resulting electric and magnetic fields evaluated on the spherical surface enclosing the particle. Eq. (3) can be further expressed as a series over the incident and scattered field coefficients [11]. All calculations are performed using standard computational methods for integral

evaluations. The trapping efficiency defined as a dimensionless factor Q is given by $Q = cF/n_2 P$, where c denotes the speed of light in vacuum, F is the trapping force and P is the incident laser power at the focus. When Q is evaluated in the transverse direction it is known as the transverse trapping efficiency (TTE), while when evaluated in the axial direction it is known as the axial trapping efficiency (ATE). We can distinguish between two ATE; the forward ATE (positive value) corresponding to the inverted microscope configuration (particle pushing) and the backward ATE (negative value) corresponding to the upright microscope configuration (particle lifting).

3. Particle size dependence and spherical aberration

Since the incident illumination on the microsphere, given in Eqs. (1) and (2), differs from the fifth-order corrected Gaussian approximation (Fig. 1(b) and 1(c)), it can be expected that the respective trapping efficiencies predicted by the our model are different. In Fig. 2(a) a comparison between the fifth-order Gaussian and vectorial diffraction approaches in the case of polystyrene particles suspended in water is presented. The Gaussian beam waist is assumed to be $\omega_0=0.4 \mu\text{m}$ while the vectorial diffraction method assumes the numerical aperture $\text{NA}=1.2$, which gives approximately the same focal spot size (Figs. 1(b) and 1(c)). For small particles both methods give nearly the same TTE and ATE, which shows an $\sim r^3$ dependence as expected for Rayleigh sized particles [18]. When their size approaches the illumination wavelength the two methods differ significantly. However, in the case of very large particles ($r=100 \mu\text{m}$.) the extrapolation of the vectorial diffraction method (dotted lines in Fig. 2(a)) approaches the RO prediction.

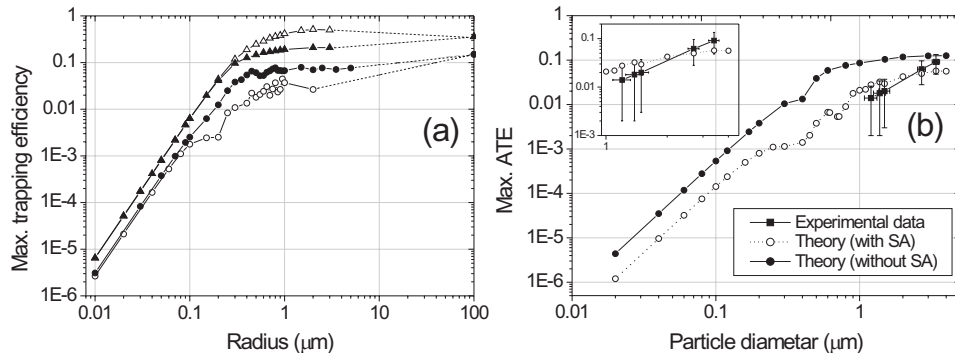


Fig. 2. (a) Comparison between the fifth-order Gaussian approximation (empty symbols) and the vectorial diffraction theory (filled symbols) for the calculation of maximal TTE (triangles) and backward ATE (circles) of polystyrene particles suspended in water. $\lambda_0=1.064 \mu\text{m}$, $\omega_0=0.4 \mu\text{m}$ and $\text{NA}=1.2$. (b) Maximal backward ATE of glass particles suspended in water, illuminated by a laser beam ($\lambda_0=1.064 \mu\text{m}$), focused by an oil immersion microscope objective ($\text{NA}=1.3$). The effect of SA is considered at a depth of $9 \mu\text{m}$ from the cover glass

SA plays an important role in laser trapping because most of the trapping experiments are performed under conditions where the refractive index mismatch occurs. Usually a high NA oil immersion objective is used for trapping while microparticles are suspended in water. The refractive index difference between the immersion and the suspending media leads to the SA when a trapping beam is focused deep into the suspending medium, which are manifested as focal spot distortions, and degrade the trapping efficiency of an optical trap.

Using the approach given in Eqs. (1) and (2), one can easily incorporate the effect of SA on trapping force at an arbitrary depth in the suspending medium. Without considering the effect of SA produced when a refractive index mismatch exist, as it does in most of the experimental measurements, one not only overestimate the value of the trapping efficiency but also lose its physical dependence on other factors such as the particle size. As it can be seen in Fig. 2(b), by including the effect of SA the calculated backward ATE agrees with the

experimental data given by Felgner *et al.* [19] under the similar condition. Furthermore, the effect of morphology dependent resonance (MDR) is pronounced for the particles whose size is of the order of wavelength in the case when SA is included. The stronger MDR effect is due to the better coupling of the incident field into the microsphere when SA is present, because the focal region is larger and the field interaction with the edge of the sphere is more pronounced.

A dependence of the trapping efficiency on the trapping distance from the cover glass, for both axial (Fig. 3(a)) and transverse (Fig. 3(b)) directions are investigated and compared with the experimental results given by Felgner *et al.* [19]. Note that the magnitude of the error bars of the experimental results depends on the trapping distance from the cover glass because the measurement of the trapping force close to the cover glass is more uncertain than that deeper into the suspending medium. In the calculation, an oil immersion objective with NA=1.3 and an illumination wavelength $\lambda_0=1.064 \mu\text{m}$ are assumed, while the refractive indices are assumed to be 1.52 for oil and cover glass (index matched), 1.57 for polystyrene, 1.51 for glass, 1.33 for water and 1.41 for 60% glycerol. The calculated maximal ATE as a function of the distance d for the trapping of a spherical glass particle of diameter $D=2.7 \mu\text{m}$ and suspended in water agrees (within its error bars) with the measured results (Fig. 3 (a)). This agreement at a large distance from the cover glass (deeper into the suspending medium) is better than that near the surface.

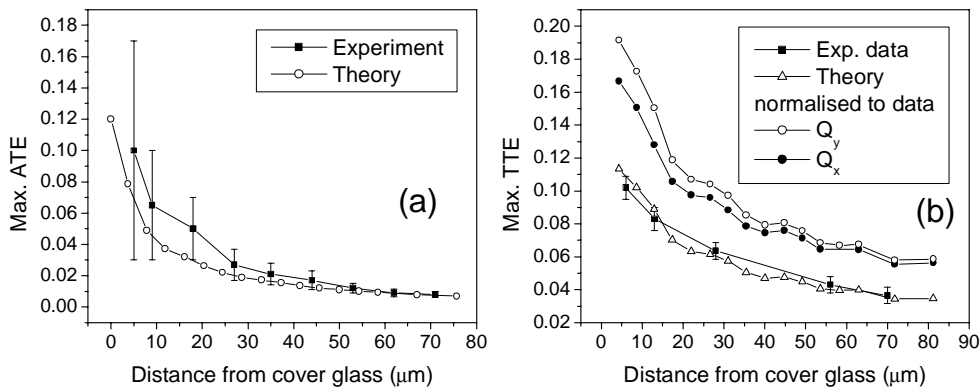


Fig. 3. Maximal backward ATE and TTE of a particle illuminated by a laser ($\lambda_0=1.064 \mu\text{m}$) focused by an oil immersion microscope objective (NA=1.3) as a function of the distance from the cover glass. (a) A glass particle of diameter $D=2.7 \mu\text{m}$ in water. (b) A polystyrene particle of diameter $D=1.02 \mu\text{m}$ suspended in a 60% glycerol solution.

Due to the asymmetry in the transverse EM field distribution in the focal region of a high NA objective (Fig. 1(b) and 1(c)), the maximal TTE in the polarization direction (Q_x) and in the direction perpendicular to the polarization direction (Q_y), calculated for a polystyrene particle of $D=1.02 \mu\text{m}$ suspended in a 60% glycerol solution, is different (Fig. 3(b)). The TTE in the Q_x direction is generally smaller than that in the Q_y direction. This difference is due to the elongation of the focal spot in the X direction. Such a difference of the TTE is larger near the surface. Although the absolute value of the TTE is slightly larger than the experimental result, which may be caused by our assumptions about the microscope objective and the suspending medium characteristics, the maximal TTE trend is consistent with the experimentally measured trend if the former is normalized by the experimental result obtained at a deep distance.

3. Trapping force mapping

According to our analysis of the dependence of the maximal trapping efficiency on particle size (Fig. 2(a)), both maximal TTE and backward ATE are greatly reduced when a particle becomes small. However, even though such presentation is related to the effect that is

measurable in the experiments, it does not give a clear physical picture of how the force depends on the relative position of the geometrical focus and the particle. Such a physical picture was presented by Ashkin *et al.* in the case of very large particles and was investigated using a RO model [10], which is not applicable for particles whose size is comparable to the illumination wavelength or smaller, and is particle size invariant. However, it could be expected that the force dependence of the relative position of the geometrical focus and the particle is markedly different for small and large particles due to the focus EM field distribution. We have considered two polystyrene particle sizes ($r=200$ nm and $r=2\mu\text{m}$) suspended in water illuminated by a $1.064\ \mu\text{m}$ laser focused using NA=1.25 water immersion objective (Figs. 4(a) and 4(b)). For large particles, the magnitude and direction of the trapping force is similar to the one given by the RO model and it is seen that the particle is most strongly influenced when its boundary is situated near the geometrical focus, while away from the boundary the trapping force falls rapidly (Fig. 4(a)). Such a rapid decrease in the trapping force magnitude is not present when dealing with small particles (Fig. 4(b)). Even at a distance of twice the particle radius, the magnitude of the trapping efficiency is relatively unchanged. This is because the particle is much smaller than the focal field distribution so that even at a geometrical focus distance of $2r$, the particle-field interaction is significant.

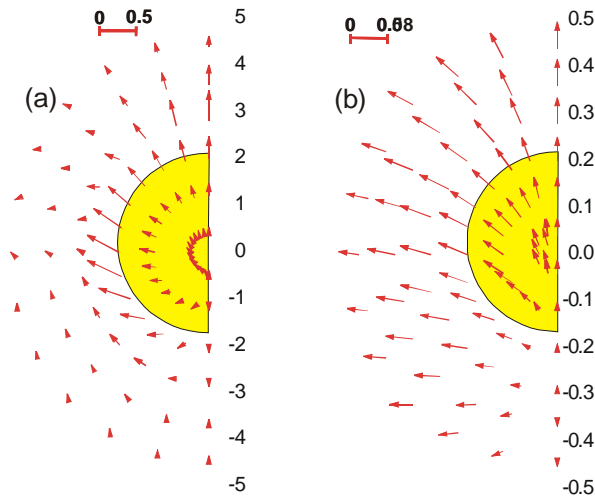


Fig. 4. Magnitude and direction of the trapping efficiency for various geometrical focus positions around a polystyrene particle suspended in water and illuminated by a $\lambda_0=1.064\ \mu\text{m}$ laser focused by a NA=1.25 water immersion objective. (a) particle radius of $2\ \mu\text{m}$. (b) Particle radius of 200 nm.

4. Conclusion

In conclusion, we have presented an exact method for the radiation trapping force calculation. The EM field distribution in the focal region of a microscope objective is determined using the vectorial diffraction theory and the optical trapping force is evaluated using the Maxwell stress tensor approach. This method offers a number of advantages over an approximate method such as the fifth-order Gaussian beam incident field approximation. It has been shown that the trapping efficiencies evaluated using our method agree well with the experimental results. Its most important significance is that it provides the appropriate treatment of the incident illumination phase modulation, polarization and apodization as well as SA occurred in trapping experiments for both small and large particles.

Acknowledgments

The authors thank the Australian Research Council for its support.